Input Shaping via B-spline Filters for 3-D Trajectory Planning

Luigi Biagiotti, Claudio Melchiorri

***Abstract*— In this paper, the equivalence between uniform B-splines of degree p and the output of a chain composed by p average filters is exploited for optimizing the trajectories used in robotic applications. In particular, the spline trajectories obtained with the proposed generator are characterized from a frequency point of view. Their frequency content is completely determined by the degree p and by the time period T between the equally-spaced knots. It is therefore possible to select these parameters with the purpose of suppressing residual vibrations, that may be present because elastic phenomena affecting the robotic system. In this sense, the proposed approach is very similar to input shaping methods and allows to find a trade-off between two different problems: on one side the requirement of exactly interpolating a set of given points by means of a complex trajectory such as a spline, on the other hand the need of suppressing mechanical vibrations. The effectiveness of the proposed approach is shown by applying it to the generation of a 3D trajectory for a cartesian robot with elastic joints.**

I. Introduction

Spline functions are extensively used in robotics in order to define smooth trajectories, especially in the workspace where interpolation of given points may result a nontrivial problem. As a matter of fact, a number of tasks performed by robots (mobile robots, industrial robots, humanoid robots, etc.) require paths with very complex shapes. Usually these profiles are defined by means of via-points, that must be interpolated or approximated with smooth functions to be optimized in order to comply with the constraints imposed by the specific robot application, i.e. kinematic constraints (such as limit values of velocity, acceleration, jerk, etc.) or dynamic constraints on the maximum torque available. Such interpolation tasks are typically performed by means of cubic splines since they assure the continuity of velocity and acceleration and prevent large oscillations of the trajectory that can result with high order polynomials, [1]. Cubic splines have been also used to minimize the total traveling time of robot trajectories subject to constraints of velocity, acceleration and jerk [2], or to globally minimize some quantities, such as acceleration [3] or jerk [4]. Conversely, to the best of authors' knowledge, an optimization of B-spline trajectories based on frequency domain considerations has never been performed before. Such kind of analysis and optimization is indeed very important when robotic systems are characterized by resonant modes that arise because of compliant elements present in the mechanical structure. In this case, a typical approach based on a proper generation of the reference input is the so-called input shaping, consisting in filtering the reference commands by convolving them with a train of impulses in order to form new commands that cause little or no vibrations [5], [6]. This technique, with some variations, has been successfully applied to a number of robotic applications, see e.g. [7], [8], [9], [10], [11], [12] among many others. However, it is worth noticing that this method aims to suppress vibrations when the input command stops but does not address the problem of maintaining the original geometric path unchanged. Moreover, it is generally limited to simple reference inputs such as step functions.

The main contribution of this paper is to provide an exact characterization of trajectories based on uniform B-splines in the frequency domain, combining the advantages of these functions, that allow to plan motions with complex geometric paths simply starting from a desired set of via-points to be interpolated/approximated, with the possibility of shaping the frequency spectrum of the motion profile by acting on the free parameters, namely the order of the B-spline curves and the distance among the knots.

L. Biagiotti is with the Department of Information Engineering, University of Modena and Reggio Emilia, Via Vignolese 905, 41100 Modena, Italy, e-mail: luigi.biagiotti@unimore.it.

C. Melchiorri is with the Department of Electronics, Informatics and Systems, University of Bologna, Viale Risorgimento 2, 40136 Bologna, Italy, e-mail: claudio.melchiorri@unibo.it.

II. B-spline filters

An important advance in the characterization of B-spline trajectories in the frequency domain is represented by [13], where the equivalence between an important class of spline curves and linear dynamic systems fed with proper input signals is demonstrated. In particular, it has been shown that trajectories based on uniform B-splines[1] of degree p can be computed by feeding a cascade of p filters

$$M(s) = \frac{1}{T}\frac{1-e^{-sT}}{s}, \tag{1}$$

shown in Fig. 1, with functions obtained as a linear combination of B-basis of degree 0 with coefficients the control points $\boldsymbol{p}_j$:

$$\boldsymbol{p}(t) = \sum_{j=0}^{n} \boldsymbol{p}_j B^0(t - jT).$$

Note that, since $B^0(t)$ is a rectangular function defined as

[1]Uniform B-spline are defined as

$$\mathbf{s}_u^p(t) = \sum_{j=0}^{n} \boldsymbol{p}_j B^p(t - jT), \qquad 0 \le t \le (m-1)T,$$

where the vectorial coefficients $\boldsymbol{p}_j$, $j = 0, \ldots, m$, called *control points*, determine the shape of the curve, $B^p(t)$ are B-spline basis functions of degree p, and T denotes the (constant) time-distance between successive knots, i.e. $t_{j+1} - t_j = T,\ j = 0, \ldots m-2$.

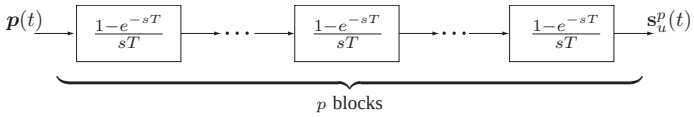

Fig. 1. System composed by p filters for the generation of trajectories based on uniform B-splines starting from the sequence of the control points $\boldsymbol{p}_j$.

$$B^0(t) = \begin{cases} 1, & \text{if } 0 \le t < T \\ 0, & \text{otherwise} \end{cases}$$

$\boldsymbol{p}(t)$ is piecewise constant that in the generic interval $jT \le t < (j+1)T$ assumes the constant value $\boldsymbol{p}_j$ of the j-th control point of the related analytic B-spline. In terms of Laplace transform, the expression of uniform B-splines based on linear filters is

$$\boldsymbol{S}_u^p(s) = \mathcal{L}\left\{\sum_{j=0}^{n} \boldsymbol{p}_j B^0(t-jT)\right\} \cdot \underbrace{M(s) \cdot M(s) \cdot \ldots \cdot M(s)}_{p \text{ filters}}. \tag{2}$$

In multidimensional B-splines, the control points $\boldsymbol{p}_j$ are multi-dimensional and the function $\boldsymbol{p}(t)$ is multidimensional as well. In this case, it is necessary to consider the different components and filter each of them with a separate chain of mean filters. For the details about the digital implementation of the trajectory generator and the methods for the computation of the control points from approximation/interpolation conditions on a given set of data points refer to [13] and [1].

III. Frequency Analysis of B-Spline Trajectories

The spectrum of the trajectory can be readily deduced by considering (2), that can be rewritten as

$$\boldsymbol{S}_u^p(s) = \boldsymbol{P}(s) \cdot M^p(s) \tag{3}$$

where $\boldsymbol{P}(s) = \mathcal{L}\left\{\sum_{j=0}^{n} \boldsymbol{p}_j B^0(t-jT)\right\}$ and $M^p(s)$ represents the transfer function of the chain of p filters $M(s)$, i.e.

$$M^p(s) = \underbrace{M(s) \cdot \ldots \cdot M(s)}_{p \text{ times}}.$$

As a matter of fact, as it is well known, the Fourier Transform of $\boldsymbol{s}_u^p(t)$ immediately descends from $\boldsymbol{S}_u^p(s)$, being its restriction to the imaginary axis, i.e. $\boldsymbol{S}_u^p(j\omega)$. Therefore, the closed form expression of $\boldsymbol{S}_u^p(j\omega)$ is given by the products of the Fourier signal corresponding to the input $\boldsymbol{p}(t)$ and the frequency response of the filters composing the trajectory generator:

$$\boldsymbol{S}_u^p(j\omega) = \boldsymbol{P}(j\omega) \cdot M^p(j\omega)$$

where

$$\begin{aligned} M^p(j\omega) &= \left(\frac{1}{T}\frac{1-e^{j\omega T}}{j\omega}\right)^p \\ &= \left(e^{-j\frac{\omega T}{2}}\frac{\sin\left(\frac{\omega T}{2}\right)}{\frac{\omega T}{2}}\right)^p. \end{aligned} \tag{4}$$

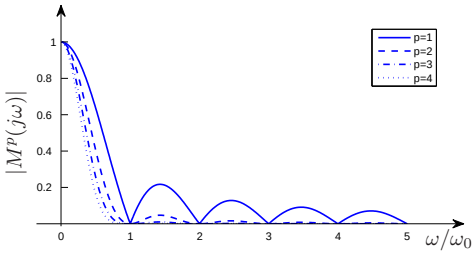

Fig. 2. Magnitude of the frequency response of the chain of filters $M^p(s)$ used for generating uniform B-spline trajectories of degree p.

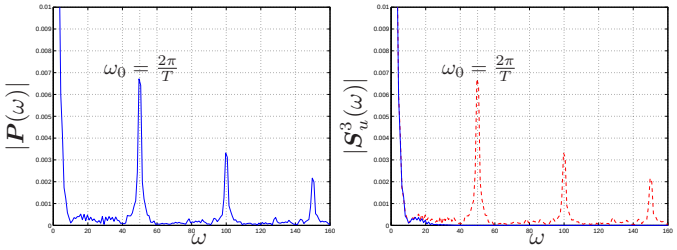

(a) (b)

Fig. 3. Frequency spectrum of a generic piecewise constant function $\boldsymbol{p}(t)$ (the x component of the control points defining the cubic B-spline trajectory considered in the next section has been assumed) with $T = 0.1257$ s, that corresponds to $\omega_0 = \frac{2\pi}{T} = 50$ rad/s, (a) and spectrum of the cubic B-spline trajectory obtained by filtering $\boldsymbol{p}(t)$ with $M^3(s)$, obtained with the same T, (b).

In particular, the magnitude of the frequency response of the cascade of p filters is given by

$$|M^p(j\omega)| = \left|\frac{\sin\left(\frac{\omega T}{2}\right)}{\frac{\omega T}{2}}\right|^p = \left|\text{sinc}\left(\frac{\omega}{\omega_0}\right)\right|^p$$

where sinc$(\cdot)$ denotes the normalized sinc function defined as $\text{sinc}(x) = \frac{\sin(\pi x)}{\pi x}$ and $\omega_0 = \frac{2\pi}{T}$. Note that the function $|M^p(j\omega)|$, shown in Fig. 2 for $p = 1, 2, 3, 4$, is equal to zero for $\omega = k\,\omega_0$, with k integer. Moreover, by augmenting the value of the degree p, the spectral components that follows the frequency ω_0 are considerably reduced. These features of the spectrum of $M^p(s)$ can be profitably exploited to properly choose the free parameter of the filter/B-spline trajectory, that is the time-distance T between the knots, with the purpose of decreasing or even nullifying the spectrum of the trajectory at critical frequencies, for instance the eigenfrequencies of the robotic manipulator.

In Fig. 3(a) the magnitude spectrum $|\boldsymbol{P}(\omega)|$ of a typical function $\boldsymbol{p}(t)$ (in particular, the x component of the control points defining the cubic B-spline trajectory considered in the next section is taken into account) is shown. Note that, since $\boldsymbol{p}(t)$ is composed by a sequence of rectangular functions of amplitude $\boldsymbol{p}_j$ and duration T s, besides the low-frequency components tied to the "average shape" of the motion profile, its spectrum has harmonic terms at frequencies multiple of $\omega_0 = \frac{2\pi}{T}$. The system $M^p(s)$ acts like a low pass filter that reduces the high frequency content of $\boldsymbol{p}(t)$ (and in particular the components at $k\,\omega_0$, k integer, where its frequency response is theoretically null). In Fig. 3(b) the magnitude

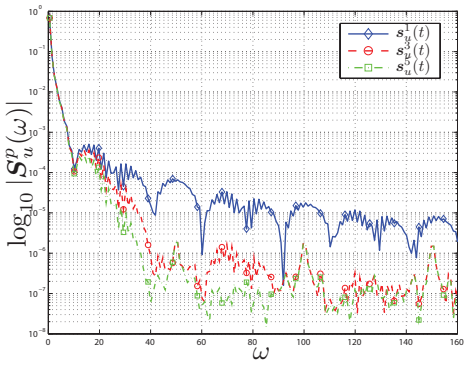

Fig. 4. Frequency spectrum of B-spline trajectories of degree p obtained by filtering the function $\boldsymbol{p}(t)$, whose spectrum is reported in Fig. 3(a), with $M^p(s)$, $p = 1, 3, 5$.

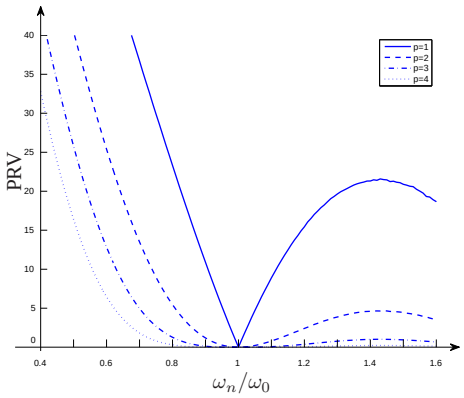

Fig. 5. Percent Residual Vibration (PRV) obtained by considering the B-spline filter $M^p(s)$, $p = 1, \ldots, 4$ as an input shaper.

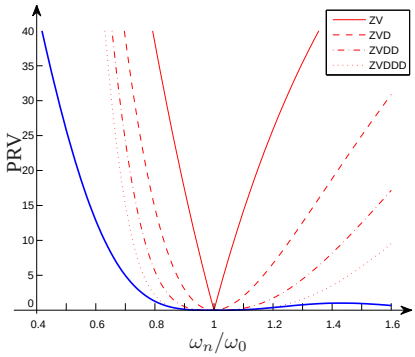

Fig. 6. Percent Residual Vibration of the cubic B-spline filter $M^3(s)$ (thick solid blue line) compared with those obtained with standard input shapers.

spectra of the input signal $\boldsymbol{p}(t)$ and of the output trajectory $\boldsymbol{s}_u^3(t)$, obtained with three filters $M(s)$, are compared. Obviously, the higher the degree p is, the stronger the attenuation of high frequency terms is, as shown Fig. 4, where the spectra of B-spline trajectories obtained for $p = 1, 3, 5$ are reported.

These considerations about the harmonic content of the B-spline trajectories obtained with the generator of Fig. 1, are particularly useful when they are applied to vibratory systems. In particular if one considers a single mode of vibration, corresponding to a single second-order linear time-invariant system with damping ratio δ and natural frequency ω_n, it is possible to evaluate the effectiveness of $M^p(s)$ in suppressing residual vibrations by considering a unitary step input $\boldsymbol{p}(t) = h(t)$ and measuring the level of vibrations at the output of the system after that the trajectory $\boldsymbol{s}_u^p(t)$ has ended (that is after $p \cdot T$ second after the application of the step). The worst case of undamped system ($\delta = 0$) is assumed in order to simplifies the estimation of the residual vibration that remains constant after the end of the motion. The results are reported in Fig. 5, where the Percent Residual Vibration (PRV[2]) obtained with $M^p(s)$, $p = 1, \ldots, 4$ is shown as a function of the normalized natural frequency ω_n/ω_0. As expected, residual vibration is null when the resonant frequency $\omega_r = \omega_n$ of the system equals ω_0. Moreover, the level of the vibration decreases with higher values of p. In Fig. 6, the PRV obtained by filtering the command input with $M^3(s)$ (that corresponds to a cubic B-spline) is compared with the PRV related to standard Input Shapers (IS), that is Zero Vibration (ZV) IS, Zero Vibration and Derivative (ZVD) IS and so on, whose expression for an undamped system is

$$C(s) = \left(\frac{1 + e^{-s\frac{\pi}{\omega_0}}}{2} \right)^p$$

where $p = 1$ corresponds to a ZV IS, $p = 2$ to a ZVD IS, etc. The levels of vibration in the neighborhood of $\omega_n = \omega_0$ for $M^3(s)$ and ZVDDD are comparable, but it is worth noticing that the PRV characteristics of the cubic B-spline filter is strongly asymmetric. This considerably augments the robustness of the filter with respect to errors in the estimation of ω_n. The insensitivity of $M^p(s)$, that is the width of the frequency range where the PRV curve is below a tolerable vibration level [6], may be easily made infinite. As a matter of fact, given a desired maximum level of vibrations V_{tol}, it is sufficient to chose the degree p large enough in order to guarantee that PRV $\leq V_{tol}$, $\forall \omega_n \geq \omega_0$. This result limits the minimum duration of the B-spline curve: given a vibratory system for which $\omega_n \geq \omega_{n,min}$, the residual vibrations may be made arbitrarily small (by acting on p) only if

$$T \geq \frac{2\pi}{\omega_{n,min}}.$$

IV. Trajectory tracking in presence of structural elasticities: B-Spline filters vs Input shapers

In order to demonstrate the effectiveness of the use of B-spline filters for vibration reduction the standard model of a robot with elasticity lumped in the joints is considered [15]:

$$\boldsymbol{M}(\boldsymbol{q})\ddot{\boldsymbol{q}} + \boldsymbol{C}(\boldsymbol{q}, \dot{\boldsymbol{q}}) + \boldsymbol{g}(\boldsymbol{q}) + \boldsymbol{K}(\boldsymbol{q} - \boldsymbol{\theta}) + \boldsymbol{D}(\dot{\boldsymbol{q}} - \dot{\boldsymbol{\theta}}) = \boldsymbol{0} \quad (5)$$

$$\boldsymbol{B}\ddot{\boldsymbol{\theta}} + \boldsymbol{K}(\boldsymbol{\theta} - \boldsymbol{q}) + \boldsymbol{D}(\dot{\boldsymbol{\theta}} - \dot{\boldsymbol{q}}) = \boldsymbol{\tau} \quad (6)$$

where $\boldsymbol{q}$ and $\boldsymbol{\theta}$ are the vectors of link positions and motor positions respectively, $\boldsymbol{M}(\boldsymbol{q})$ ($\boldsymbol{B}$) is the inertia matrix of

[2]According to [14] Percent Residual Vibration is defined as the ratio of the residual vibration from the command shaped by $M^p(s)$ to the residual vibration to the step command.

i	m_i	d_i	k_i
x	2.777 kg	4 N/m s	1e+4 N/m
y	6.25 kg	4 N/m s	1e+4 N/m
z	2.777 kg	4 N/m s	1e+4 N/m

TABLE I
ROBOT PARAMETERS.

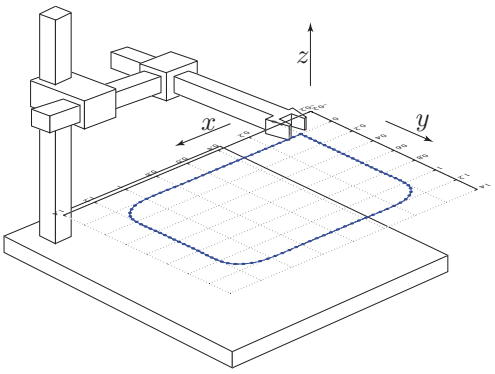

Fig. 7. Cartesian Robot tracking a planar trajectory defined by a set of via-points.

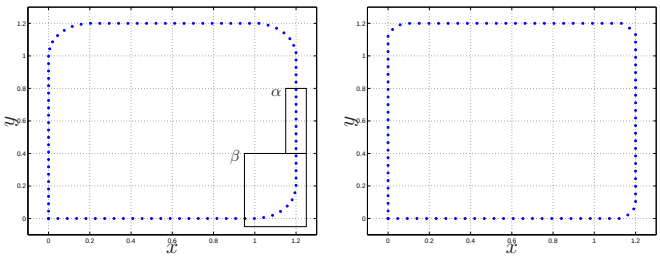

(a) (b)

Fig. 8. Via-points $\boldsymbol{q}_i$ defining the trajectory in the 2D space: low curvature bends (a) and high curvature bends (b). α and β denote two regions used for evaluation of the trajectory, in terms of residual vibrations induced into the system and tracking errors.

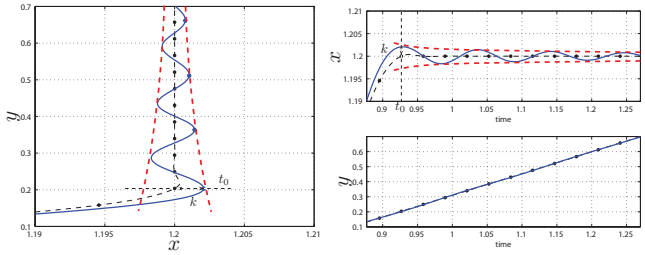

(a) (b)

Fig. 9. Measurement of residual vibration affecting x-axis: geometric path (a) and motion profiles as a function of time (b).

the robot (actuators), $\boldsymbol{C}(\boldsymbol{q}, \dot{\boldsymbol{q}})$ denotes the Coriolis and centrifugal terms, $\boldsymbol{g}(\boldsymbol{q})$ takes into account the gravity effects and $\boldsymbol{K}$, $\boldsymbol{D}$ are the stiffness and the damping matrices of the transmission system. For the sake of simplicity, a cartesian structure is taken into account, equipped with an ideal controller able to impose to the actuators the desired trajectories $\boldsymbol{q}_d$ without errors, that is $\boldsymbol{\theta} \equiv \boldsymbol{q}_d$. In this way, the model (5) becomes

$$\boldsymbol{M}\ddot{\boldsymbol{q}} + \boldsymbol{D}\dot{\boldsymbol{q}} + \boldsymbol{K}\boldsymbol{q} = \boldsymbol{D}\dot{\boldsymbol{q}}_{\boldsymbol{d}} + \boldsymbol{K}\boldsymbol{q}_d \tag{7}$$

where $\boldsymbol{M} = \text{diag}\{m_i\}$, $\boldsymbol{D} = \text{diag}\{d_i\}$, $\boldsymbol{K} = \text{diag}\{k_i\}$, $i = x, y, z$, and $\boldsymbol{q} = (x, y, z)^T$, $\boldsymbol{q_d} = (x_d, y_d, z_d)^T$. Therefore, along the different axes, the robot behaves as an ideal second-order system characterized by a natural frequency and a damping ratio

$$\omega_{n,i} = \sqrt{\frac{k_i}{m_i}}, \qquad \delta_i = \frac{d_i}{2\sqrt{k_i\, m_i}}.$$

The values of the parameters considered in the simulations are reported in Tab. I. They lead to $\omega_n = 60$ rad/s and $\delta = 0.012$ along x and z axes, while in the y direction $\omega_n = 40$ rad/s and $\delta = 0.008$. For the sake of generality, different values of the dynamic parameters are considered along the different axes. As shown in Fig. 7, a 2-D trajectory lying in the $x - y$ plane has been considered.

The geometric path is composed by straight lines with circular bends and is defined by means of a sequence of equally-spaced via-points $\boldsymbol{q}_i$, see Fig. 8. In particular, two curves are considered, that differ in the curvatures of the bends. These particular paths have been assumed because the circular bends allow to evaluate the capability of the system of exactly tracking the trajectory and because the residual vibration can be easily estimated along the straight line segments. The residual vibration affecting the x-axis is measured from the envelope of the oscillations about the y-axis, as shown in Fig. 9. For such oscillations, it is conventionally assumed an initial time-instant t_0 that coincides with the interpolation time-instant of the first via-point of the straight line segment. Dually, the residual vibration related to the y-axis is measured when the robot moves in the x direction. Since the amplitude of the oscillations is clearly proportional to the magnitude of the input (in this case, both the B-spline filter, or the input shaper, and the robotic manipulator are linear systems), the values of residual vibration are normalized, by dividing them by the average distance between the via points ($d = \text{mean}(\text{dist}(\boldsymbol{q}_i, \boldsymbol{q}_{i+1})) \approx 0.0454$ m) and a percent value is considered (this value is called Residual Vibration (RV)).

In Fig. 10 the residual vibrations in the x and y directions consequent to the application of a uniform B-spline filter of degree 3 are reported. The filter is applied to the sequence of control points $\boldsymbol{p}_j$, determined from the via-points $\boldsymbol{q}_i$ according to the algorithm reported in [13]. The simulative results confirm the considerations of previous section: the residual vibration remains limited until ω_0 does not overcome the natural frequency of the plant. In this case, one should assume $\omega_0 \leq \min\{\omega_{n,x}, \omega_{n,y}\} = 40$ rad/s (and therefore $T \geq 2\pi/\min\{\omega_{n,x}, \omega_{n,y}\}$). The choice of B-spline curves of higher degree allows to decrease the level of vibrations in the overall frequency range and in particular within the interval $[0, \omega_n]$, as illustrated in Fig. 11, where the residual vibrations for different values of p are reported for both the curves defined in Fig. 8. The same conclusions can be drawn from an analysis of the trajectory in the $x - y$ plane. For instance in Fig. 12 the residual vibrations about the x axis are shown for different values of ω_0 and p. In the case

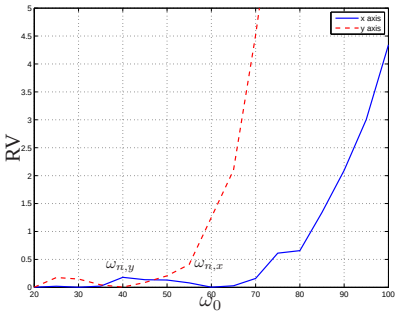

Fig. 10. Residual vibration with a cubic B-spline along x and y directions.

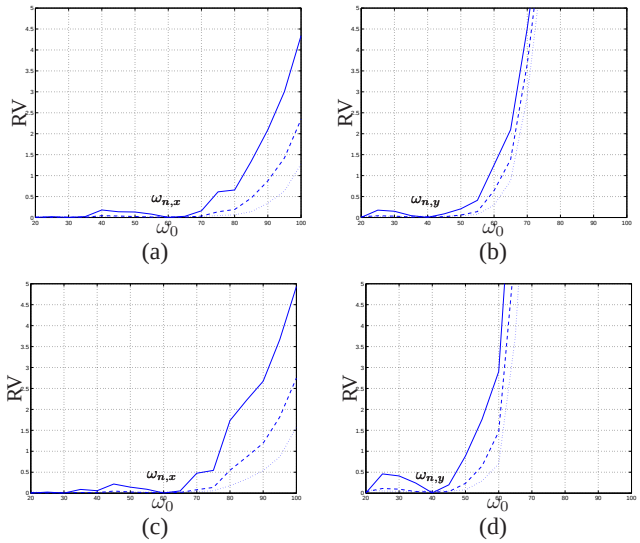

Fig. 11. Residual vibration for the B-spline trajectories of Fig. 8(a) (a)-(b), and Fig. 8(b) (c)-(d), along x and y axes respectively ($p = 3$ solid line, $p = 4$ dashed line, $p = 5$, dotted line).

$\omega_0 = 40$ rad/s, the response to the cubic B-spline exhibits some (small) oscillations, that disappear for $p = 4$ or 5. In general, the vibrations are smaller for higher values of p.

The behavior of B-spline filters is compared with that of input shapers in order to highlight the pros and cons of the two techniques. A first important difference consists in the fact that input shapers receive as input the via-points $\boldsymbol{q}_i$ to be interpolated, without the need of computing the control points $\boldsymbol{p}_j$. Moreover, they can be designed independently from the time-distance T between the points. For this reason the IS are set with $\omega_0 = 50$ rad/s and the effect of T on the residual vibrations affecting the movement of the robotic manipulator are analyzed. As illustrated in Fig. 13, where the ZV IS and the ZVDD IS are taken into account, the residual vibrations are considerably reduced for high values of p, but the value of ω_0, intermediate value between $\omega_{n,x}$ and $\omega_{n,y}$, leads to large oscillations for $T = 2\pi/\omega_{n,x}$ and $T = 2\pi/\omega_{n,y}$, respectively in the x and in the y direction. On the other hand, one can observe that the time T is not limited (from below) by $2\pi/\min\{\omega_{n,x}, \omega_{n,y}\}$.

If one designs the IS with two different values of ω_0 ($\omega_{0,x} = \omega_{n,x} = 60$ rad/s and $\omega_{0,y} = \omega_{n,y} = 40$ rad/s),

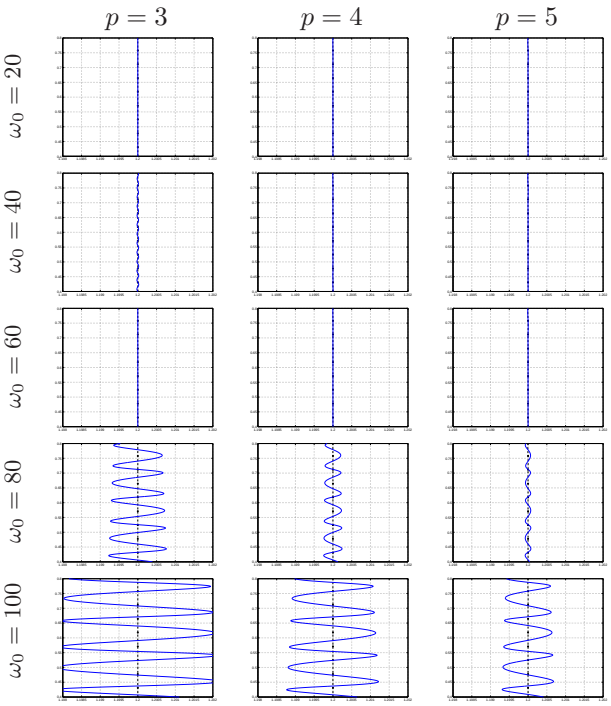

Fig. 12. Residual vibration for B-spline trajectories about the x axis: detail of the geometric path that in Fig. 9(a) is denoted with α.

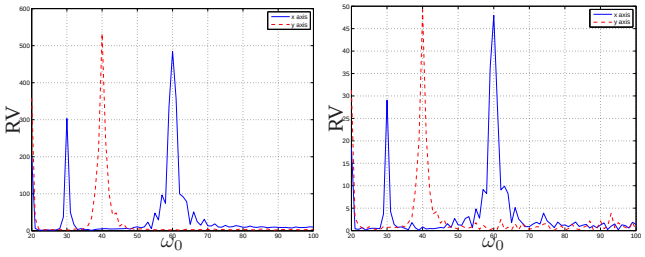

Fig. 13. Residual vibration for the trajectory of Fig. 8(a) filtered by a ZV IS (a) and a ZVDD IS (b) (designed with $\omega_0 = 50$ rad/s).

as shown in Fig. 14, the peaks of residual vibrations can be further reduced. Nevertheless, it is worth noticing that also in this ideal case IS are not able to guarantee the exact interpolation of the given via-points. In Fig. 15 a detail of the trajectories obtained with ZV IS and ZVDD IS is reported. Note that both the output of the IS (dashed red line) and the trajectory performed by the robot (solid blue line) do not cross the points $\boldsymbol{q}_i$. On the contrary, B-spline trajectories interpolate the points $\boldsymbol{q}_i$, as shown in Fig. 16.

As a last remark, it is necessary to highlight that, although a bit conservative, the condition that guarantee a low level of residual vibrations for B-spline filters

$$T \geq \frac{2\pi}{\omega_n}$$

requires only a rough estimation of the natural frequency ω_n of the flexible mode that affects the plant. This is very important for applications involving robot with elastic elements, since multiple vibratory modes may be present (as

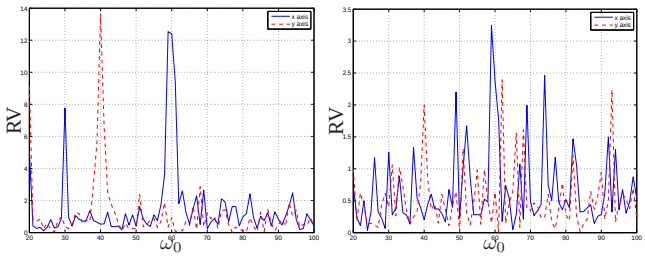

(a) (b)

Fig. 14. Residual vibration for the trajectory of Fig. 8(a) filtered by a ZV IS (a) and a ZVDD IS (b) (designed with $\omega_{0,x} = 60$ rad/s and $\omega_{0,y} = 40$ rad/s).

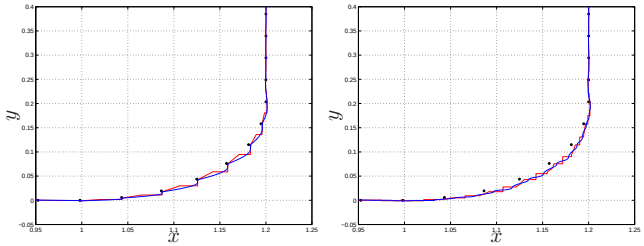

(a) (b)

Fig. 15. Detail of the trajectory in the $x - y$ plane obtained by filtering the via-points with ZV IS (a) and ZVDD IS (b)(designed with $\omega_{0,x} = 60$ rad/s and $\omega_{0,y} = 40$ rad/s).

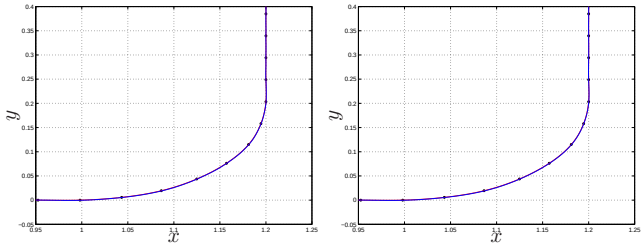

(a) (b)

Fig. 16. Detail of the trajectory in the $x - y$ plane obtained with B-spline filters of degree $p = 3$ (a) and $p = 5$ (b) (designed with $\omega_0 = 50$ rad/s).

in this example), and in general the natural frequency is not constant but it is a function of the robot configurations $\boldsymbol{q}$ [16], [15]. In this case, one must simply assume

$$T \geq \frac{2\pi}{\min_{\boldsymbol{q}}\{\omega_n(\boldsymbol{q})\}}.$$

V. Conclusions

The equivalence between analytical uniform B-splines of degree p and the output of a chain composed by p mean filters fed with piecewise constant functions provides a precise characterization of such kind of trajectories in the frequency domain. The simple expression of their frequency spectrum allows a straightforward optimization of B-spline trajectories in terms of degree p and of time period T between the equally-spaced knots (that determines the duration of the movement). This approach, very similar to input shaping, is particularly useful in order to suppress vibrations when plants with vibratory modes are considered, but at the same time it offers the possibility of planning complex trajectories that interpolates desired sequences of via-points. Moreover, the considerations on the spectrum of B-spline trajectories provide an estimation of the minimum value of their duration as a function of the dynamic behavior of the system that must track the trajectory (resonant frequency) and not on the basis of the kinematic/dynamic limits of the actuation system (maximum velocity, acceleration or torque).
The example, relating to a 3-D trajectory applied to a cartesian robot with elastic joints, shows the effectiveness of the proposed method.

References

[1] L. Biagiotti and C. Melchiorri, *Trajectory Planning for Automatic Machines and Robots*, 1st ed. Heidelberg, Germany: Springer, 2008.

[2] C.-S. Lin, P.-R. Chang, and J. Luh, "Formulation and optimization of cubic polynomial joint trajectories for industrial robots," *IEEE Transaction on Automatic Control*, vol. 28, no. 12, pp. 1066–1074, 1983.

[3] B. Cao, G. Dodds, and G. Irwin, "Constrained time-efficient and smooth cubic spline trajectory generation for industrial robots," *Proceedings of IEE Conference on Control Theory and Applications*, vol. 144, pp. 467–475, 1997.

[4] A. Piazzi and A. Visioli, "Global minimum-jerk trajectory planning of robot manipulator," *IEEE Transaction on Industrial Electronics*, vol. 47, no. 1, pp. 140–149, 2000.

[5] N. C. Singer and W. P. Seering, "Preshaping command inputs to reduce system vibration," *ASME Journal of Dynamic Systems, Measurement, and Control*, vol. 112, pp. 76–82, 1990.

[6] J. Vaughan, A. Yanoa, and W. Singhose, "Comparison of robust input shapers," *Journal of Sound and Vibration*, vol. 315, no. 4-5, pp. 797–815, 2008.

[7] D. Magee and W. Book, "Implementing modified command filtering to eliminate multiple modes of vibration," in *American Control Conference, 1993*, San Francisco, CA, USA, 2-4 June 1993, pp. 2700 – 2704.

[8] ——, "Optimal filtering to minimize the elastic behavior in serial link manipulators," in *American Control Conference, 1998. Proceedings of the 1998*, vol. 5, Philadelphia, PA , USA, 21-26 Jun 1998, pp. 2637 – 2642.

[9] H.-S. Park, P. Chang, and J.-S. Hur, "Time-varying input shaping technique applied to vibration reduction of an industrial robot," in *Intelligent Robots and Systems, 1999. IROS '99. Proceedings. 1999 IEEE/RSJ International Conference on*, vol. 1, Kyongju , South Korea, 17 ott - 21 ott 1999, pp. 285 – 290.

[10] S. k. Yun, S. Kang, M. Kim, and S.-S. Yoon, "Input preshaping control of the safe arm with mr-based passive compliant joints," in *Robotics and Automation, 2004. Proceedings. ICRA '04. 2004 IEEE International Conference on*, vol. 3, 26 April-1 May 2004, pp. 2788 – 2793.

[11] J. Park, P.-H. Chang, H.-S. Park, and E. Lee, "Design of learning input shaping technique for residual vibration suppression in an industrial robot," *Mechatronics, IEEE/ASME Transactions on*, vol. 11, no. 1, pp. 55 – 65, 2006.

[12] N. Chang, N. Chang, T. Chang, and E. Hou, "High speed position control of a swinging load," in *Industrial Electronics (ISIE), 2010 IEEE International Symposium on*, Bari, Italy, 4-7 July 2010, pp. 190 – 195.

[13] L. Biagiotti and C. Melchiorri, "B-spline based filters for multi-point trajectories planning," in *2010 IEEE International Conference on Robotics and Automation*, Anchorage, Alaska, May 3-8 2010.

[14] K. Kozak, W. Singhose, and I. Ebert-Uphoff, "Performance measures for input shaping and command generation," *Journal of Dynamic Systems Measurement and Control*, vol. 128, no. 3, pp. 731–736, 2006.

[15] A. D. Luca and W. Book, *Springer Handbook of Robotics*. Berlin: Springer Verlag, 2008, ch. Robots with Flexible Elements, pp. 287–317.

[16] J. A. Somolinos, V. Feliu, and L. Snchez, "Design, dynamic modelling and experimental validation of a new three-degree-of-freedom flexible arm," *Mechatronics*, vol. 12, no. 7, pp. 919 – 948, 2002.